# Effect of Argon or Helium on the $CO_2$ Conversion in a Dielectric Barrier Discharge

Marleen Ramakers,* Inne Michielsen, Robby Aerts, Vera Meynen, Annemie Bogaerts*

This paper demonstrates that the $CO_2$ conversion in a dielectric barrier discharge rises drastically upon addition of Ar or He, and the effect is more pronounced for Ar than for He. The effective $CO_2$ conversion, on the other hand, drops upon addition of Ar or He, which is logical due to the lower $CO_2$ content in the gas mixture, and the same is true for the energy efficiency, because a considerable fraction of the energy is then consumed into ionization/excitation of Ar or He atoms. The higher absolute $CO_2$ conversion upon addition of Ar or He can be explained by studying in detail the Lissajous plots and the current profiles. The breakdown voltage is lower in the $CO_2$/Ar and $CO_2$/He mixtures, and the discharge gap is more filled with plasma, which enhances the possibility for $CO_2$ conversion. The rates of electron impact excitation–dissociation of $CO_2$, estimated from the electron densities and mean electron energies, are indeed higher in the $CO_2$/Ar and (to a lower extent) in the $CO_2$/He mixtures, compared to the pure $CO_2$ plasma. Moreover, charge transfer between $Ar^+$ or $Ar_2^+$ ions and $CO_2$, followed by electron-ion dissociative recombination of the $CO_2^+$ ions, might also contribute to, or even be dominant for the $CO_2$ dissociation. All these effects can explain the higher $CO_2$ conversion, especially upon addition of Ar, but also upon addition of He.

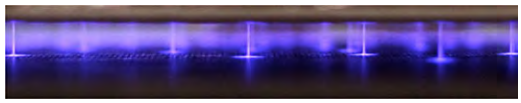

## 1. Introduction

In recent years, there is increased interest in $CO_2$ splitting by plasma, to produce CO and $O_2$.[1–16] Thermodynamically, this reaction requires a lot of energy (i.e., 2.9 eV/molec or 279.8 kJ/mol), which would typically be supplied in classical processes by heating the gas. In a non-thermal plasma, however, the gas can remain at room temperature, because energetic electrons are created, which can activate the gas by electron impact excitation, ionization, and dissociation. Different types of plasmas have been applied for $CO_2$ conversion, but most research is carried out with either dielectric barrier discharges (DBDs),[2–10] microwave plasmas,[11–13] and gliding arc discharges.[14–16] Although microwave and gliding arc plasmas are more promising in terms of energy efficiency, DBD plasmas have other advantages such as operating at atmospheric pressure, a simple design, and easy upscaling capabilities.[17] Moreover, they can be combined with a catalyst, to improve the selectivity towards targeted products, when mixing $CO_2$ with another gas, such as $CH_4$, $H_2$, or $H_2O$, for the production of value-added chemicals.[18–22]

A large number of experiments have been performed already in pure $CO_2$,[2–16] but also mixed with $CH_4$,[18–21] $H_2$,[22–24] or $H_2O$,[25–27] to form value-added chemicals. Moreover, a few papers have reported on the mixing of $CO_2$ (and $CH_4$) with a rare gas, such as He or Ar.[28–31] Pinhao et al.[28] investigated $CO_2$/$CH_4$/He mixtures in a DBD and observed that the addition of He results in a drop in the breakdown voltage and it enhances the conversion of both $CO_2$ and $CH_4$. On the other hand, the range of stable discharge operating conditions was

M. Ramakers, I. Michielsen, R. Aerts, V. Meynen, A. Bogaerts
Department of Chemistry, University of Antwerp, Universiteitsplein 1, Wilrijk-Antwerp B-2610, Belgium
E-mail: marleen.ramakers@uantwerpen.be; annemie.bogaerts@uantwerpen.be




DOI: 10.1002/ppap.201400213

reduced. Also Gouilard et al.[29] reported that He dilution yields higher conversions of $CO_2$ and $CH_4$ in a DBD, which they attributed to Penning ionization. Lindon et al.[30] compared a DBD operating in pure $CO_2$ and in a 60/40 $CO_2$/Ar mixture, and found that the $CO_2$ conversion and energy efficiency were greatly improved upon addition of Ar, and they suggested that this was due to a reduction in the plasma breakdown voltage and an increase in the $CO_2^+$ population, due to charge exchange with argon ions. Finally, Ozkan et al.[31] investigated the conversion of $CO_2$ and $CH_4$ in a DBD with multi-electrodes and observed an increase in conversion of both $CO_2$ and $CH_4$ upon addition of Ar or He. They explained this effect due to the difference of the shape of the electron energy distribution function (EEDF) when the plasma is in the filamentary regime (Ar) or in the glow regime (He). Thus, the nature of the carrier gas – and consequently the regime (glow or filamentary) of the DBD – directly impacts the shape of the EEDF and therefore the electron collision processes that may occur.

However, to our knowledge, no systematic studies on the effects of He or Ar addition on the $CO_2$ conversion, including more detailed attempts to explain the behavior based on the underlying mechanisms, have been reported yet.

In the present paper, we will therefore systematically investigate the effect of Ar and He addition on the $CO_2$ conversion and on the energy efficiency in a DBD reactor over a broad concentration range, and we will try to explain the observed effects by detailed electrical characterization of the plasma.

## 2. Experimental Set-up

The experiments were performed with a cylindrical DBD reactor, illustrated in Figure 1. It consists of a stainless-steel rod with a diameter of about 12.88 mm and length of 200 mm, which acts as inner electrode and is grounded, surrounded by a dielectric tube, made of $Al_2O_3$, with (more or less) the same length, and an outer and inner diameter of 22 and 16.54 mm. The distance between the inner electrode and the dielectric tube, i.e., the so-called discharge gap, is 1.83 mm. The dielectric tube is surrounded by the outer electrode, made of nickel foil, powered by a high voltage supply. The length of the outer electrode is 90 mm, so this defines the length of the plasma.

The high voltage is supplied by a generator and transformer (AFS). The applied voltage is measured with a high voltage probe (Tek P6015A), while a Rogowski coil (Pearson 4100) is used to measure the total current. Moreover, the voltage on an external capacitor (10 nF) is measured to obtain the generated charges (Q) in the plasma. Plotting Q as a function of the applied voltage (U) gives us a Q-U Lissajous plot, as will be demonstrated below. Finally, all electrical signals are recorded by an oscilloscope (PicoScope 6402 A).

The input gas flow of $CO_2$, Ar, and He is controlled by thermal mass flow controllers (Bronkhorst), and the gas at the outlet is analyzed by a compact GC (Interscience). The total gas flow rate is always kept constant at 300 mL/min, and the $CO_2$, Ar and He fractions are varied between 5% and 95%. Furthermore, measurements in pure $CO_2$ are also carried out. For each GC measurement, 10 samples are taken, of which only the last five are used, to ensure stabilization of the gas composition. First, blank measurements are taken, i.e., without plasma. Subsequently, a power of 80 W is applied, with a frequency of 23.5 kHz, and after half an hour, i.e., when the measured voltage is more or less constant, GC measurements are taken, to define the $CO_2$ conversion as follows:

$$X_{CO_2}(\%) = \frac{CO_{2(in)} - CO_{2(out)}}{CO_{2(in)}} \times 100\%$$

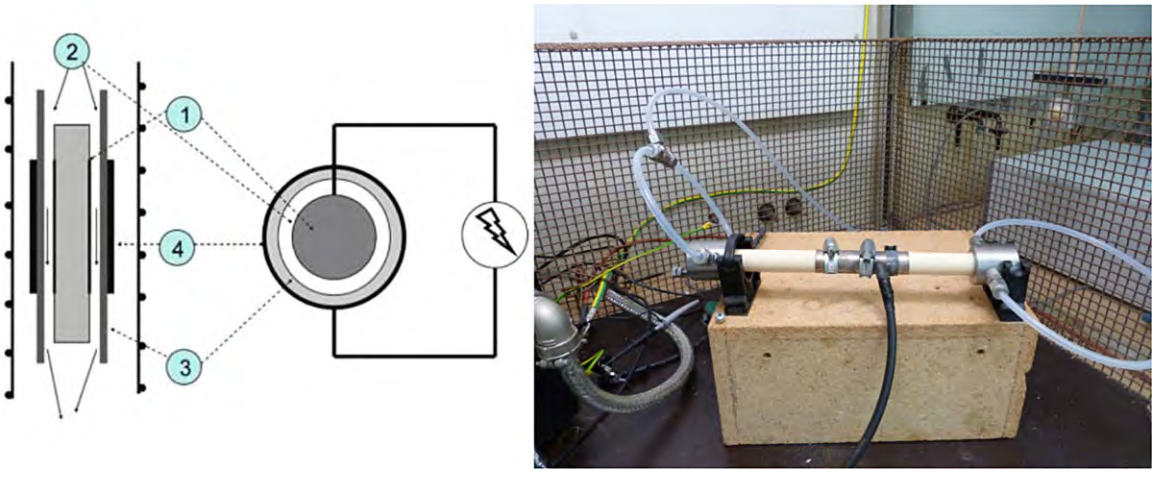


*Figure 1.* Left: schematic diagram of the cylindrical DBD reactor, with 1 = inner electrode, 2 = discharge gap, 3 = dielectric tube, 4 = outer electrode. Right: picture of the DBD reactor.



DOI: 10.1002/ppap.201400213

where $CO_{2(in)}$ and $CO_{2(out)}$ are the $CO_2$ signals without and with plasma, respectively.

## 3. Results and Discussion

### 3.1. Effect of Ar and He on the $CO_2$ Conversion and Energy Efficiency

As mentioned above, the experiments are carried out in pure $CO_2$ and with the addition of Ar or He, in the range between 5% and 95%. Figure 2 shows the $CO_2$ conversion as a function of $CO_2$ fraction in the gas mixture, for both Ar and He addition. It is clear that the conversion is lowest, i.e., around 5%, in the pure $CO_2$ plasma, and increases drastically upon addition of either Ar or He. At low Ar or He fractions, and up to 70%, the effect of Ar and He is very similar, with the He addition giving slightly higher conversion. However, at Ar or He fractions above 70%, the effect becomes most pronounced for Ar addition, where a conversion of 41% is reached in the 5/95 $CO_2$/Ar gas mixture, whereas in the 5/95 $CO_2$/He mixture, the conversion is around 25%.

Although the conversion of $CO_2$ increases upon addition of Ar or He, it is important to note that the effective amount of $CO_2$ that is converted, will drop from about 5.5% (in pure $CO_2$) to 2% upon addition of 95% Ar, and even to 1.2% in the case of adding 95% He. The reason is simply because there is less $CO_2$ present in the gas mixture that can be converted. This is illustrated in Figure 3. The effective amount of $CO_2$ converted is used to calculate the energy efficiency of this process. The following formulas are used for this purpose:

$$\eta(\%) = \frac{\Delta H_R\left(\frac{kJ}{mol}\right) * X_{CO_2 eff}(\%)}{SEI\left(\frac{kJ}{L}\right) * 22.4\left(\frac{L}{mol}\right)}$$

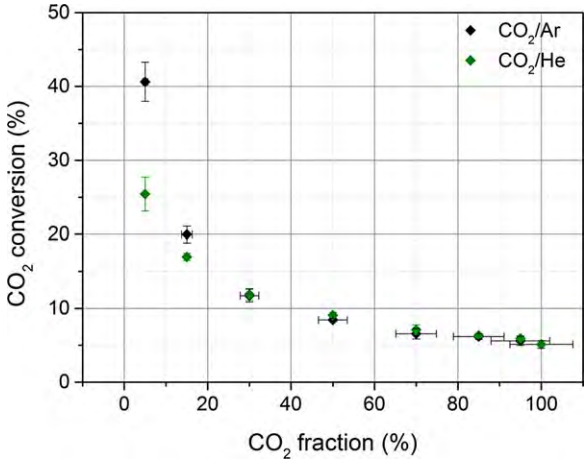


*Figure 2.* $CO_2$ conversion as a function of $CO_2$ fraction in $CO_2$/Ar and $CO_2$/He gas mixtures, at an applied power of 80 W and a frequency of 23.5 kHz.

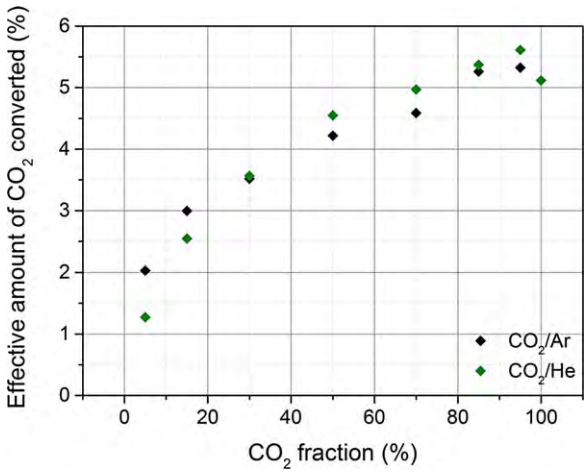


*Figure 3.* Effective amount of $CO_2$ converted as a function of $CO_2$ fraction in $CO_2$/Ar and $CO_2$/He gas mixtures, at the same conditions as in Figure 2.

where $\Delta H_R$ is the reaction enthalpy of $CO_2$ splitting (i.e., 279.8 kJ/mol; see Introduction), $X_{CO_2, eff}$ is the effective amount of $CO_2$ converted, and SEI is the specific energy input in the plasma, defined as:

$$SEI\left(\frac{kJ}{L}\right) = \frac{Plasma\ power(kW)}{Flow\ rate\left(\frac{L}{min}\right)} \times 60\left(\frac{S}{min}\right)$$

where the flow rate is 300 mL/min (kept constant; see section 2 above). For the power in the above formula, in most experiments the power coupled into the plasma is adopted, i.e., the so-called plasma power. This value was obtained here for each gas composition, by means of the Lissajous figures (see below). The values varied between 37 and 43 W for $CO_2$/Ar and between 38 and 44 W for $CO_2$/He.

In Figure 4 the energy efficiency of $CO_2$ splitting is plotted as a function of $CO_2$ fraction in the gas mixture. We see that the energy efficiency rises from 1–2% at 5% $CO_2$ in the $CO_2$/Ar or $CO_2$/He mixture, respectively, to about 9% above 80% $CO_2$ in the gas mixtures. The reason that the energy efficiency is higher when more $CO_2$ is present, is simply because the effective $CO_2$ conversion is higher; hence the energy is more effectively used for $CO_2$ splitting, whereas at the lower $CO_2$ concentrations a significant fraction of the energy is also consumed by ionization/excitation of the Ar or He gas. Although some of this energy will be indirectly used for $CO_2$ dissociation, through the Ar or He ions or excited atoms, as will be elaborated below, still a considerable fraction of this energy does not lead to $CO_2$ splitting.

Note that the values obtained (up to 9% in the case of high $CO_2$ gas fractions) are typical for a DBD reactor, or even somewhat higher than commonly reported.[8,9] However, these values only reflect the energy efficiency of the plasma reactor itself. If the applied power (i.e., 80 W in our case)

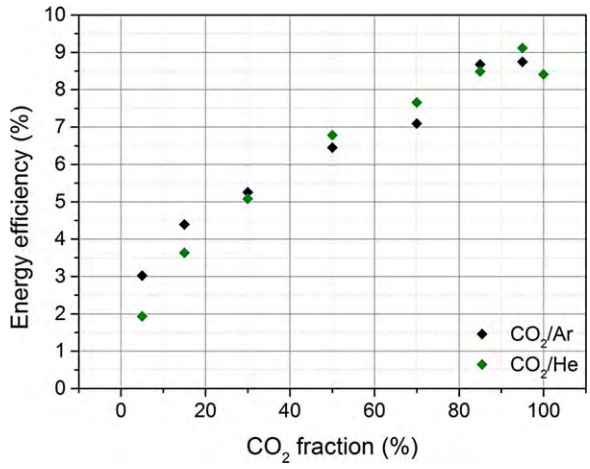


*Figure 4.* Energy efficiency of $CO_2$ splitting as a function of $CO_2$ fraction in $CO_2$/Ar and $CO_2$/He gas mixtures, at the same conditions as in Figure 2.

would be used in the above equation instead of the plasma power, the energy efficiency would reflect the overall efficiency of the setup, including also the power supply. In that case, the energy efficiency would be roughly a factor of 2 lower, because about 50% of the energy of the power supply is not used for the plasma, but is lost by heating of the electrical connections and transformer coils. Moreover, a zero load power requirement of 40 W is always consumed by the power source, making higher electrical powers (e.g., 800 W) more efficient compared to low powers such as 80 W.

### 3.2. Effect of Ar and He on the Breakdown Voltage

To explain the higher $CO_2$ conversion upon addition of Ar or He, we analyze the Lissajous-figures, which is a common method for the investigation of dielectric barrier discharges.[20,32–34] In Figure 5 we show the Lissajous plots for pure $CO_2$ and the two gas mixtures with 5% $CO_2$. The explanation of the Lissajous plot is given in the right panel of Figure 5. Lines DA and CB represent the phase when no plasma is formed; the slope of these lines indicates the total capacity of the reactor without plasma ($C_{cell}$). Note that the latter can also be theoretically estimated from the capacity of the dielectric ($C_d$) and the gap ($C_g$):

$$\frac{1}{C_{cell}} = \frac{1}{C_d} + \frac{1}{C_g}$$

These two capacities can be calculated as follows:[34]

$$C_g = \frac{2\pi\epsilon_0\epsilon_g l}{\ln(r_{inner}/r_{rod})}$$

$$C_d = \frac{2\pi\epsilon_0\epsilon_d l}{\ln(r_{outer}/r_{inner})}$$

where $\epsilon_o$, $\epsilon_g$, and $\epsilon_d$ are the permittivity in vacuum, the relative permittivity of the gas (which should be in the order of 1, for the different gases and gas mixtures[35]) and the relative permittivity of the dielectric (taken as 9.34 for $Al_2O_3$[36]), respectively. Furthermore, l is the length of the discharge zone (90 mm; see above), and $r_{inner}$, $r_{outer}$, and $r_{rod}$ are the inner and outer radii of the dielectric tube (i.e., 8.27 and 11 mm) and the radius of the inner electrode rod (6.44 mm), respectively. This yields $C_g$ in the order of 20 pF (depending on the exact value of $\epsilon_g$) and $C_d = 163$ pF. As we don't know the exact value of $\epsilon_g$, $C_g$ is subject to some uncertainties, and therefore we have directly determined $C_{cell}$ from the Lissajous plots. The obtained values for both pure $CO_2$ and for the $CO_2$/Ar and $CO_2$/He gas mixtures are listed in Table 1. It is clear that the slopes of the lines DA and CB are very similar for pure $CO_2$ and for the $CO_2$/Ar and $CO_2$/He gas mixtures, which is logical when looking at the

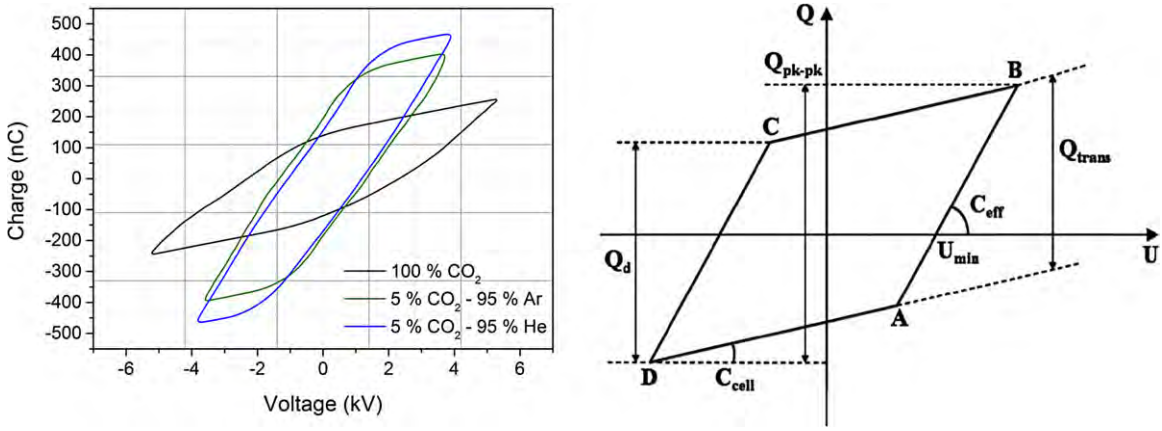


*Figure 5.* Left: Lissajous plots of the pure $CO_2$ plasma, and the plasma in a $CO_2$/Ar and $CO_2$/He mixture with 5% $CO_2$. The other conditions are the same as in Figure 1. Right: Explanation of the information that can be deduced from a Lissajous plot.


*Plasma Process. Polym.* **2015,** *12*, 755–763

DOI: 10.1002/ppap.201400213

*Table 1.* Electrical characteristics of the pure $CO_2$ plasma and the $CO_2$/Ar and $CO_2$/He gas mixtures with 5% $CO_2$, as deduced from the Lissajous plots in Figure 5.

| Gas mixture | $C_{cell}$ [pF] | $C_{eff}$ [pF] | $U_{min}$ [kV] | $U_B$ [kV] |
|---|---|---|---|---|
| 100% $CO_2$ | 21 | 73 | 2.31 | 2.06 |
| 5% $CO_2$–95% Ar | 23 | 161 | 1.32 | 1.18 |
| 5% $CO_2$–95% He | 23 | 160 | 1.18 | 1.05 |

theoretical formulas, because $C_d$ is the same and $C_g$ will only be slightly different (depending only on the exact value for $\epsilon_g$).

The lines AB and DC in Figure 5 represent the phase when the plasma is formed inside the gap, so the slope of these lines indicates the effective capacity of the plasma reactor ($C_{eff}$), which is also listed in Table 1. When the gap is entirely filled with plasma (i.e., micro discharge filaments or homogenous plasma), $C_{eff}$ would be equal to $C_d$.[20] The effect of He and Ar on the effective plasma capacity will be described in section 3.3 below.

Finally, the breakdown voltage ($U_B$) can be calculated from:

$$U_B = \frac{1}{1 + (C_g/C_d)} U_{\min}$$

where $U_{min}$ is the minimum voltage, which is deduced from the intersection of the line AB with the X-axis at Q = 0 in the Lissajous plot (see Figure 5). Both $U_{\min}$ and $U_B$ are also listed in Table 1. We see that $U_{min}$ drops upon addition of Ar or He. This also leads to a drop in $U_B$. The voltage needed to initiate the plasma will thus be lower in the $CO_2$/Ar and $CO_2$/He mixtures than in the pure $CO_2$ plasma. A similar observation was made by Pinhao et al. for a $CH_4$/$CO_2$/He DBD.[28]

The drop in $U_B$ can partially be explained by the Townsend ionization coefficient $\alpha$, which is expressed as:[1]

$$\frac{\alpha}{p} = A \exp\left(-\frac{B}{E/p}\right)$$

The parameters A and B for $CO_2$, Ar and He in the range of E/p = 30–500 V/(cm Torr)[1] are listed in Table 2. The corresponding value for $\alpha$, estimated with this formula for E/p = 100 V/(cm Torr) and 1 atm pressure, is also given in the table. We see that $\alpha$ is significantly larger for Ar and He than for $CO_2$. Moreover, we expect that the value of $\alpha$ is even overestimated in the case of $CO_2$, as this simple formula might not take into account electron attachment, which takes place in an electronegative gas like $CO_2$, and which would lower the value of $\alpha$. The same behavior can be observed for other values of E/p. This explains the lower breakdown voltage for Ar and He, as a larger value for $\alpha$ yields more electron production per unit length, so that a lower voltage can be sufficient to initiate the plasma.

The lower breakdown voltage in Ar and He can also be explained by the lower probability for inelastic collisions. Indeed, in Ar and He, electron impact excitation and ionization are the only possible inelastic collisions, and they are characterized by rather high threshold energies (i.e., 15.76 and 11.55 eV for ionization and excitation of Ar, and even 24.59 and 19.8 eV for ionization and excitation of He). On the other hand, for $CO_2$, the threshold for inelastic collisions is much lower, i.e., 6.23 eV for electronic excitation, 5.52 eV for dissociation, and only 0.08 eV for vibrational excitation to the lowest vibrational levels. Furthermore, as many vibrational levels can be excited, there are many more possibilities for the electrons to participate in inelastic collisions in $CO_2$ than in Ar or He. Moreover, the probability for recombination of electrons with $Ar^+$ or $He^+$ ions is also much lower than for recombination with $CO_2{}^+$ ions, because of the absence of dissociative recombination. In conclusion, the lower probability of the electrons for inelastic collisions with Ar or He, on one hand, and for recombination with $Ar^+$ or $He^+$ ions, on the other hand, results in a longer mean free path of the electrons in the Ar or He plasma. Hence, the electrons have more time to become accelerated in the applied electric field, so that lower voltages are sufficient for electrical breakdown.

As the plasma power in our experiments is more or less the same for the pure $CO_2$ plasma and the $CO_2$/Ar and $CO_2$/He mixtures (i.e., around 40 W; see above), this means that more power can be used for dissociation of $CO_2$, as less power will be dissipated for the gas breakdown. We believe that this is one of the reasons for the higher $CO_2$ conversion upon addition of Ar or He. A similar explanation was also recently given by Lindon et al.[30]

### 3.3. Effect of He and Ar on the Plasma Capacity

As explained in previous section, from the Lissajous plots, we can also deduce the capacities of the different gas mixtures with and without plasma (see Table 1 above). As mentioned above, $C_{cell}$ is almost the same for the different cases, which can be expected from the theoretical formulas, because $C_d$ is the same and $C_g$ will only be slightly different (depending on the exact value for $\epsilon_g$). The effective capacity

*Table 2.* Parameters A and B for the semi-empirical calculation of the Townsend ionization coefficient $\alpha$ [1], and corresponding values of $\alpha$, calculated for E/p = 100 V/(cm torr) and 1 atm pressure.

| GAS | $A\left(\frac{1}{cm \cdot Torr}\right)$ | $B\left(\frac{V}{cm \cdot Torr}\right)$ | $\alpha$ ($cm^{-1}$) |
|---|---|---|---|
| $CO_2$ | 20 | 466 | 142 |
| Ar | 12 | 180 | 1488 |
| He | 3 | 34 | 1602 |

of the plasma, on the other hand, rises significantly upon addition of either Ar or He, as is clear from Table 1, and moreover, these values become comparable to the value of $C_d$ (i.e., 163 pF) for the $CO_2$/Ar and $CO_2$/He gas mixtures. This indicates that the discharge gap will be more "filled with plasma," i.e., either as a homogenous plasma, like in the case of He, or with a higher density of micro discharge filaments, like in the case of Ar. This also explains why the dissociation of $CO_2$ will be higher in the $CO_2$/Ar and $CO_2$/He gas mixtures compared to pure $CO_2$.

### 3.4. Effect of Ar and He on the Electrical Current Profiles

Figure 6 illustrates the current profiles for pure $CO_2$ and the $CO_2$/Ar and $CO_2$/He gas mixtures with 5% $CO_2$. It is clear that in the case of the $CO_2$/Ar mixture, both the intensity of the current peaks, as well as the amplitude of the (more or less) sinusoidal current profile are significantly higher than in the case of pure $CO_2$. Hence, there will be more charges generated in the $CO_2$/Ar plasma, as could also be deduced from the Lissajous plots (cf. Figure 5 above). In the case of the $CO_2$/He mixture, the current peaks are not higher, but there is a clear rise in the amplitude of the (more or less) sinusoidal current profile, and hence also a rise in the generated charges (cf. the Lissajous plots). Note that the current profile of the $CO_2$/He mixture clearly indicates that the plasma is more homogeneous (i.e., less filamentary) than the two other discharges.

### 3.5. Effect of Ar and He on the Electron Density, Mean Electron Energy and $CO_2$ Dissocation Rate

It has been demonstrated by Aerts et al.[10] that electron impact dissociation, mainly through excitation ($e^- + CO_2 \rightarrow e^- + CO_2^* \rightarrow e^- + CO + O$) is the most important reaction for $CO_2$ splitting in a DBD. Therefore, to further explain the effect of Ar and He addition on the $CO_2$ conversion, it is interesting to compare the electron density and electron energy, as well as the rate of this electron impact excitation process, between the pure $CO_2$ plasma and the $CO_2$/Ar and $CO_2$/He gas mixtures.

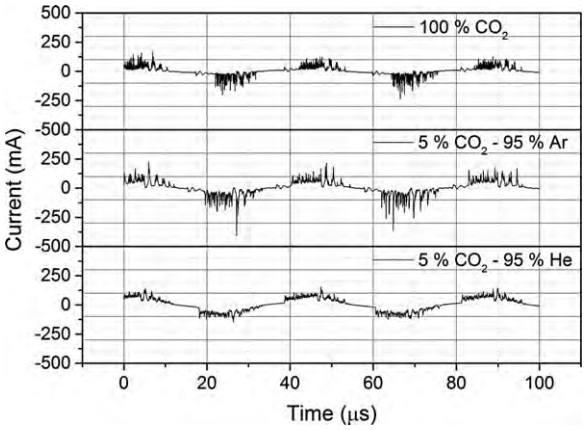


*Figure 6.* Electrical current profiles in the pure $CO_2$ plasma, and in the $CO_2$/Ar and $CO_2$/He plasmas with 5% $CO_2$, for the same conditions as in Figure 2.

We can estimate the electron density from the current profiles shown in Figure 6, by:

$$n_e = \frac{J}{E\mu_e e}$$

where $J$ is the current density, $E$ is the electric field, $\mu_e$ is the electron mobility and $e$ is the elementary charge. The value of the electric field is taken from E/n = 200 Td, which is a typical value for a DBD,[1,10] and $\mu_e$ is calculated with Bolsig +[37] for the different gas mixtures at E/n = 200 Td. The current density is estimated from the maximum current (deduced from Figure 6), divided by the surface of one micro discharge (roughly assumed to be $1.05 \times 10^{-6}$ m$^2$).[34] Note that in the case of the $CO_2$/He gas mixture, the discharge is more uniform, so the concept of the surface of a micro discharge is only a rough approximation, but this formula yields only a rough estimate of the electron density anyway. The electron densities for the pure $CO_2$ plasma and the $CO_2$/Ar and $CO_2$/He mixtures, obtained in this way, are given in Table 3. We see that the electron density is more than a factor two higher in the $CO_2$/Ar mixture, but it is a factor three lower in the $CO_2$/He mixture, compared to the pure $CO_2$ plasma. We have to point out that this method is only a rough estimation because of the three following reasons: 1) the current is measured in a situation where many filaments act simultaneously and this is not completely representing the properties of a single discharge, 2) the non-uniformity of plasma formation is suggesting that filaments with different properties are generated, 3) the discharge cross section and local electric field are dependent on the gas mixture.

The mean electron energy for the three cases, as calculated with Bolsig + , is plotted as a function of E/n in Figure 7(a). It is clear that the mean electron energy rises faster in the $CO_2$/He and $CO_2$/Ar mixture than in the pure $CO_2$ plasma. This can be explained because the electrons do not lose their energy so rapidly by inelastic collisions, because of the higher thresholds for inelastic collisions with Ar and He, as discussed above. The effect is much more pronounced in the $CO_2$/He mixture, because the thresholds for He are much higher than for Ar (see above).

Figure 7(b) illustrates the rate constants for the above-mentioned electron impact excitation of $CO_2$, leading to dissociation, as a function of E/n, also calculated with Bolsig + for the three cases. The rate constants for the pure $CO_2$ plasma



DOI: 10.1002/ppap.201400213

*Table 3.* Electron density, obtained from the current profiles of Figure 6, mean electron energy and rate constant for $CO_2$ excitation, leading to dissociation, calculated with Bolsig + for a reduced electric field of 200 Td, and corresponding rate of this reaction, for the pure $CO_2$ plasma and the $CO_2$/Ar and $CO_2$/He plasmas with 5% $CO_2$.

| Gas mixture | Electron density [$m^{-3}$] | Mean electron energy [eV] | Rate constant [$m^3/s$] | Reaction rate [$s^{-1}$] |
|---|---|---|---|---|
| 100% $CO_2$ | $6.52 \times 10^{18}$ | 6.61 | $1.8 \times 10^{-16}$ | 1200 |
| 5% $CO_2$–95% Ar | $1.64 \times 10^{19}$ | 7.83 | $2.7 \times 10^{-16}$ | 4500 |
| 5% $CO_2$–95% He | $2.05 \times 10^{18}$ | 15.43 | $1.8 \times 10^{-15}$ | 3700 |

and the $CO_2$/Ar mixture show a very similar profile, but the values in the $CO_2$/He mixture are significantly higher. This is logical, because of the higher electron energy in the $CO_2$/He plasma. Indeed, this electron excitation process, leading to $CO_2$ dissociation, requires 11.9 eV, which is higher than the mean electron energies in the pure $CO_2$ and $CO_2$/Ar plasma, so only the tail in the electron energy distribution will be able to participate in this process.

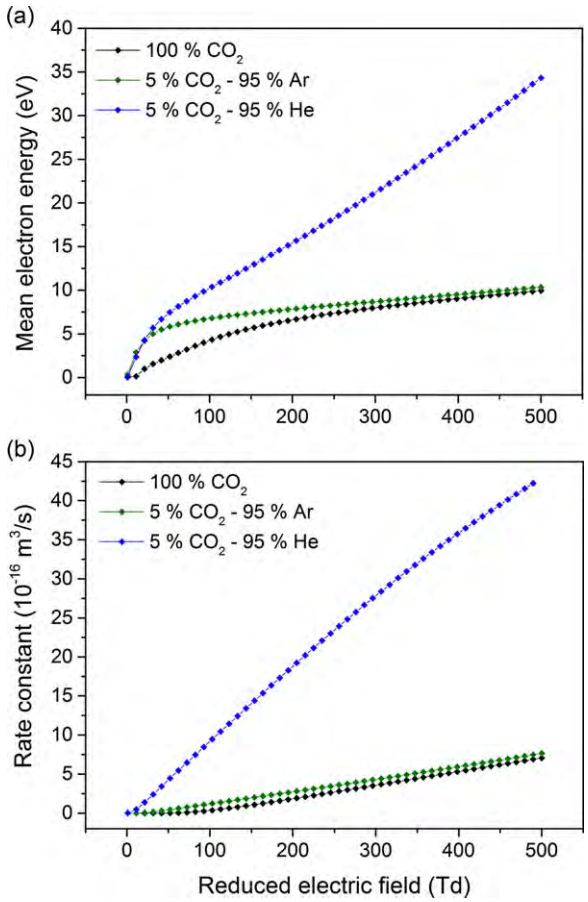


*Figure 7.* Mean electron energy (a) and rate constant for electron impact excitation of $CO_2$, leading to dissociation (b), in the pure $CO_2$ plasma, and in the $CO_2$/Ar and $CO_2$/He plasmas with 5% $CO_2$, as a function of the reduced electric field, calculated with Bolsig +.

Table 3 summarizes, besides the values of the electron density, also the mean electron energy, the rate constant for this $CO_2$ excitation–dissociation process, and the resulting rate of this reaction, calculated for E/n = 200 Td, which is a typical value for a DBD plasma (see above), for the pure $CO_2$ plasma and the $CO_2$/Ar and $CO_2$/He mixtures. As mentioned above, the electron density rises upon addition of Ar, and drops upon addition of He. The mean electron energy increases upon addition of Ar, and more drastically upon addition of He, and the same is of course true for the rate constant of $CO_2$ excitation–dissociation (cf. also Figure 7), because it depends on the mean electron energy. The product of this rate constant with the electron density gives us the electron impact excitation–dissociation rate, which is indeed higher in the $CO_2$/Ar and $CO_2$/He mixtures than in the pure $CO_2$ plasma, explaining the higher $CO_2$ conversion, shown in Figure 2 above. Moreover, the rate is higher in the $CO_2$/Ar mixture than in the $CO_2$/He mixture, explaining also why the $CO_2$ conversion is higher upon addition of Ar than upon addition of He, at least for Ar and He fractions above 70% (see Figure 2 above).

Finally, besides the above explanation, we have to keep in mind that in the $CO_2$/Ar and $CO_2$/He mixtures, some other reactions might be responsible for $CO_2$ dissociation as well. Indeed, it is stated in literature[38,39] that the addition of Ar has a beneficial effect on the $CO_2$ dissociation, because of charge transfer of the $Ar^+$ ions with $CO_2$, yielding $CO_2^+$ ions ($Ar^+ + CO_2 \rightarrow Ar + CO_2^+$). The latter can undergo dissociative electron-ion recombination ($CO_2^+ + e^- \rightarrow CO + O$), effectively contributing to $CO_2$ splitting. Alternatively, as the above charge transfer reaction is exothermic ($\Delta H = -2$ eV), it occurs quickly,[1] and the excess energy can be coupled into the vibrational and rotational states of the $CO_2$ molecule, thereby also increasing the dissocation rate.

We can estimate the rate of this charge transfer reaction, based on rate coefficients found in literature.[40–42] Typical values for this charge transfer reaction are reported to be $7.6 \times 10^{-10}$ $cm^3 s^{-1}$,[40] 4.6–$7.6 \times 10^{-10}$ $cm^3 s^{-1}$,[41] and 4.4–$7.6 \times 10^{-10}$ $cm^3 s^{-1}$[42] for $Ar^+$ ions. Moreover, a similar charge transfer reaction is also reported for $Ar_2^+$ ions, with typical rate coefficients of $1.1 \times 10^{-9}$ $cm^3 s^{-1}$[40] and $4.8 \times 10^{-10}$ –$1.1 \times 10^{-9}$ $cm^3 s^{-1}$.[42] In all cases, the

formation of $CO_2^+$ ions is reported. It is well possible that the $Ar_2^+$ ion density is (much) higher than the $Ar^+$ density at these atmospheric pressure conditions.[43] In any case, we expect that in the $CO_2$/Ar mixture with 5% $CO_2$, the highest ion density is either $Ar^+$ or (most probably) $Ar_2^+$, and its value will be in the same order as the electron density, listed in Table 3 above, i.e., $1.64 \times 10^{19}$ m$^{-3}$ (or $1.64 \times 10^{13}$ cm$^{-3}$). Multiplying this ion density with the above-mentioned rate coefficients for charge transfer, gives us an estimated rate for this process in the range between 7,220 and 18,000 s$^{-1}$, which is clearly higher than the estimated rate for electron impact excitation–dissociation, listed in Table 3 (i.e., 4,500 s$^{-1}$ at a reduced electric field of 200 Td). This suggests indeed that this charge transfer reaction is predominant for $CO_2$ dissociation in $CO_2$/Ar mixtures, and it therefore explains why the $CO_2$ conversion increases upon addition of Ar in the $CO_2$/Ar mixture.

Note that a similar reaction could in principle occur in the $CO_2$/He mixture as well, but the $He^+/He_2^+$ ion density will be lower (as can also be deduced from the lower electron density; see Table 3), because of the higher ionization potential of He (24.59 eV vs. 15.76 eV for Ar). Typical values for symmetric charge transfer with $He^+$ ions are reported to be $1.1 \times 10^{-9}$ cm$^3$ s$^{-1}$[40] (with a branching ratio of 79/11/10/1 toward $CO^+$, $CO_2^+$, $O^+$, and $O_2^+$ ions) and $1.2 \times 10^{-9}$ cm$^3$ s$^{-1}$[41] (forming mainly $CO^+$ and $O^+$). For $He_2^+$ ions, a value of $1.8 \times 10^{-9}$ cm$^3$ s$^{-1}$ is reported,[40] mainly forming $CO_2^+$ ions. Even if this reaction does not always form $CO_2^+$ ions, it will still contribute to $CO_2$ dissociation. Hence, following the same reasoning as above for Ar, we can multiply the electron density (as a measure for the $He^+$ or $He_2^+$ ion density) with these reported charge transfer rate coefficients, and this yields a rate in the order of 2,255–3,690 s$^{-1}$. This value is significantly lower than the rate for charge transfer in Ar, due to the lower $He^+/He_2^+$ ion densities, but it is comparable (or slightly lower) than the estimated rate for electron impact excitation–dissociation in the $CO_2$/He mixture (i.e., 3,700 s$^{-1}$ at the reduced electric field of 200 Td; see Table 3), indicating that this process might indeed also play a role, albeit probably not so dominant as in the $CO_2$/Ar mixture.

Finally, it is worth to mention that Penning ionization of $CO_2$ by He or Ar excited levels, yielding $CO_2^+$ ions, or a so-called Penning dissociation reaction by He or Ar excited levels, might also play a role in the enhanced $CO_2$ dissociation upon addition of Ar or He, as was suggested in.[29] However, as we don't have data on the densities of the He or Ar excited levels at the investigated conditions, we cannot quantify the importance of these processes.

## 4. Conclusions

We have performed a rather detailed electrical characterization of a DBD plasma operating in $CO_2$ and in $CO_2$/Ar and $CO_2$/He mixtures, to explain why the $CO_2$ conversion rises drastically upon addition of Ar or He, and why the effect is more pronounced for Ar than for He, at least for Ar or He gas fractions above 70%. From the Lissajous plots it is clear that the breakdown voltage is significantly lower in the $CO_2$/Ar and $CO_2$/He mixtures, which suggests that a larger fraction of the applied power can be used effectively for the $CO_2$ conversion. Moreover, the effective capacity of the plasma is higher in the $CO_2$/Ar and $CO_2$/He mixtures, and becomes comparable to the capacity of the dielectric, indicating that the discharge gap is more filled with plasma (either due to more energy dense micro discharge filaments in $CO_2$/Ar, or by a homogeneous plasma in $CO_2$/He), which enhances also the possibility for $CO_2$ conversion. Finally, the Lissajous plots illustrate that more charges are generated in the $CO_2$/Ar and $CO_2$/He mixtures, which can also be observed from the electrical current profiles.

The electron densities are estimated from these current profiles, and the electron mean energies are calculated with Bolsig + , as well as the rate constants for electron impact excitation of $CO_2$, which is the most important process responsible for $CO_2$ dissociation in a DBD. The product of the electron densities and the rate constants gives us the rates of electron impact excitation–dissociation of $CO_2$, which are indeed higher, especially in the $CO_2$/Ar mixture, but also in the $CO_2$/He mixture, compared to the pure $CO_2$ plasma. Moreover, in the $CO_2$/Ar mixture, a charge transfer process between $Ar^+$ or $Ar_2^+$ ions and $CO_2$, followed by electron-ion dissociative recombination of the $CO_2^+$ ions, will most probably also contribute to the $CO_2$ dissociation, and it might even be the dominant process, as suggested by the estimated rates. In principle, this effect can take place with $He^+$ or $He_2^+$ ions as well, but the $He^+/He_2^+$ ion density is expected to be (significantly) lower than the $Ar^+/Ar_2^+$ density, based on the higher ionization potential, and as can be deduced from the electron densities. All these effects can explain the higher $CO_2$ conversion upon addition of Ar or He, and can also explain why the $CO_2$ conversion is higher in the $CO_2$/Ar mixtures than in the $CO_2$/He mixtures at $CO_2$ concentrations below 30%.

Finally, it is worth to mention that the effective $CO_2$ conversion, which indicates how much $CO_2$ is effectively converted, keeping in mind the $CO_2$ concentration in the mixture, drops upon addition of Ar or He, and the same is true for the energy efficiency, which is calculated from the effective $CO_2$ conversion. Indeed, at lower $CO_2$ fractions in the gas mixtures, a larger fraction of the energy will be consumed by the Ar or He gas, and only part of it (through the Ar or He ions or excited atoms) will be finally used for $CO_2$ conversion.

Acknowledgments: The authors acknowledge financial support from two IOF-SBO projects of the University of Antwerp, and the


*Plasma Process. Polym.* **2015,** *12*, 755–763

DOI: 10.1002/ppap.201400213

IAP/7 (Inter-university Attraction Pole) program "PSI-Physical Chemistry of Plasma-Surface Interactions" by the Belgian Federal Office for Science Policy (BELSPO) and from the Fund for Scientific Research Flanders (FWO).

Received: November 5, 2014; Revised: December 19, 2014; Accepted: January 3, 2015; DOI: 10.1002/ppap.201400213

Keywords: argon; $CO_2$ splitting; conversion; dielectric barrier discharges (DBD); helium

[1] A. Fridman, *Plasma Chemistry*, Cambridge University Press, Cambridge **2008**.
[2] J. Wang, G. Xia, A. Huang, S. L. Suib, Y. Hayashi, *H. J. Catal.* **1999**, *185*, 152.
[3] K. Jogan, A. Mizuno, T. Yamamoto, *J. IEEE Trans Industry Applic.* **1993**, *29*, 876.
[4] G. Zheng, J. Jiang, Y. Wu, R. Zhang, H. Hou, *Plasma Chem. Plasma Process.* **2003**, *23*, 59.
[5] R. Li, Y. Yamaguchi, S. Yin, Q. Tang, T. Sato, *Solid State Ionics* **2004**, *172*, 235.
[6] R. Li, Q. Tang, S. Yin, T. Sato, *Fuel Process. Technol.* **2006**, *87*, 617.
[7] S. Paulussen, B. Verheyde, X. Tu, C. De Bie, T. Martens, D. Petrovic, A. Bogaerts, B. Sels, *Plasma Sources Sci. Technol.* **2010**, *19*, 034015.
[8] S. Wang, Y. Zhang, X. Liu, X. Wang, *Plasma Chem. Plasma Process.* **2012**, *32*, 979.
[9] Q. Yu, M. Kong, T. Liu, J. Fei, X. Zheng, *Plasma Chem. Plasma Process.* **2012**, *32*, 153.
[10] R. Aerts, T. Martens, A. Bogaerts, *J. Phys. Chem. C* **2012**, *116*, 23257.
[11] L. Maya, *J. Vac. Sci. Technol. A* **2000**, *18*, 285.
[12] M. Tsuji, T. Tanoue, K. Nakano, Y. Nishimura, *Chem. Lett.* **2001**, *1*, 22.
[13] L. F. Spencer, A. D. Gallimore, *Plasma Sources Sci. Technol.* **2013**, *22*, 015019.
[14] A. Indarto, J. Choi, H. Lee, H. K. Song, *Environ. Eng. Sci.* **2006**, *23*, 1033.
[15] A. Indarto, D. R. Yang, J.-W. Choi, H. Lee, H. K. J. Song, *Hazard Mater.* **2007**, *146*, 309.
[16] T. Nunnally, K. Gutsol, A. Rabinovich, A. Fridman, A. Gutsol, A. J. Kemoun, *Phys. D Appl. Phys.* **2011**, *44*, 274009.
[17] U. Kogelschatz, *Plasma Chem. Plasma Process.* **2003**, *23*, 1.
[18] M. Kraus, B. Eliasson, U. Kogelschatz, A. Wokaun, *Phys. Chem. Chem. Phys.* **2001**, *3*, 294.
[19] Q. Wang, B. H. Yan, Y. Jin, Y. Cheng, *Energy & Fuels* **2009**, *23*, 4196.
[20] X. Tu, H. J. Gallon, M. V. Twigg, P. A. Gorry, J. C. J. Whitehead, *Phys. D Appl. Phys.* **2011**, *44*, 274007.
[21] H. J. Gallon, X. Tu, J. C. Whitehead, *Plasma Process. Polym.* **2012**, *9*, 90.
[22] A. Bill, A. Wokaun, B. Eliasson, E. Killer, U. Kogelschatz, *Energy Convers. Mgmt* **1997**, *38*, S415.
[23] B. Eliasson, U. Kogelschatz, B. Xue, L.-M. Zhou, *Ind. Eng. Chem. Res.* **1998**, *37*, 3350.
[24] M. Kano, G. Satoh, S. Iizuka, *Plasma Chem. Plasma Process.* **2012**, *32*, 177.
[25] S. Futamura, H. Kabashima, in *Carbon Dioxide Utilization for Global Sustainability, Proceedings of the 7th International Conference on Carbon Dioxide Utilization*, Elsevier, Amsterdam **2004**. Vol. *153*, p. 119.
[26] T. Ihara, M. Kiboku, Y. Iriyama, *Bull. Chem. Soc. Japan* **1994**, *67*, 312.
[27] T. Ihara, T. Ouro, T. Ochiai, M. Kiboku, Y. Iriyama, *Bull. Chem. Soc. Japan* **1996**, *69*, 241.
[28] N. R. Pinhão, A. Janeco, J. B. Branco, *Plasma Chem. Plasma Process.* **2011**, *31*, 427.
[29] V. Goujard, J.-M. Tatibouët, C. Batiot-Dupeyrat, *Plasma Chem. Plasma Process.* **2011**, *31*, 315.
[30] M. A. Lindon, E. E. Scime, *Front. Phys.* **2014**, *2*, 1.
[31] A. Ozkan, T. Dufour, G. Arnoult, P. De Keyzer, A. Bogaerts, F. Reniers, *J. $CO_2$ Util.* In press.
[32] S. Liu, M. Neiger, *J. Phys. D Appl. Phys* **2003**, *36*, 3144.
[33] A. V. Pipa, T. Hoder, J. Koskulics, M. Schmidt, R. Brandenburg, *Rev. Sci. Instrum.* **2012**, *83*, 075111.
[34] R. Valdivia-Barrientos, J. Pacheco-Sotelo, M. Pacheco-Pacheco, J. S. Benítez-Read, R. López-Callejas, *Plasma Sources Sci. Technol.* **2006**, *15*, 237.
[35] D. R. Lide, *CRC Handbook of Chemistry and Physics*, 85th edition, CRC Press, Boca Raton **2004**.
[36] K. F. Young, H. P. R. Frederikse, *J. Phys. Chem. Ref. Data* **1973**, *2*, 313.
[37] G. J. M. Hagelaar, L. C. Pitchford, *Plasma Sources Sci. Technol.* **2005**, *14*, 722.
[38] K. Hensel, S. Katsura, A. Mizuno, *IEEE Trans Plasma Sci.* **2005**, *33*, 574.
[39] S. L. Suib, S. L. Brock, M. Marquez, J. Luo, H. Matsumoto, Y. J. Hayashi, *Phys. Chem. B* **1998**, *102*, 9661.
[40] D. L. Albritton, *Atom. Data Nucl. Data Tables* **1978**, *22*, 1.
[41] E. Ferguson, *Atom. Data Nucl. Data Tables* **1973**, *12*, 159.
[42] R. J. Shul, B. L. Upschulte, R. Passarella, R. G. Keesee, A. W. Castleman, Jr, *J. Phys. Chem.* **1987**, *91*, 2556.
[43] W. Van Gaens, A. Bogaerts, *J. Phys. D: Appl. Phys.* **2013**, *46*, 275201.